

## THE INFLUENCE OF MULTICELLULAR MERIDIONAL FLOWS IN SETTING THE CYCLE PERIOD IN SOLAR DYNAMO MODELS

Jouve Laurène and Brun Allan Sacha<sup>1</sup>

**Abstract.** Inspired by recent observations and 3D simulations that both exhibit multicellular meridional circulation flows in the solar convection zone, we seek to characterize the influence of such multiple flows in setting the magnetic solar cycle period. For most existing mean field dynamo models of flux transport type, the flow is assumed to be constituted of a large single cell per meridional quadrant extending from the surface (where it is poleward) to slightly below the core-envelope interface (where it is equatorward). Here we study the influence of adding meridional cells both in latitude and in radius. We confirm that 2 cells in latitude speeds up the cycle but we find on the contrary that 2 cells in radius significantly increases the cycle period.

### 1 Introduction

The Sun is believed to possess both a global and a local dynamo which is the source of its intricate magnetic activity (Brun et al. 2004). Mean field models are very useful numerical tools to study global solar dynamo (Charbonneau 2005; Dikpati & Charbonneau 1999). In particular, these models can be used to study the establishment of the butterfly diagram, the cycle period, the phase relationship between the poloidal and toroidal fields. In mean field dynamo models, two effects are thought to be at the origin of dynamo action, the  $\Omega$  and  $\alpha$  effects. The  $\Omega$  effect is now constrained by helioseismology (Thompson et al. 2003) and thus has lead the community to reconsider the reference mean field dynamo model. The favored models today are of flux transport type, assuming both a source of poloidal field at the surface (a Babcock-Leighton source term) and at the bottom ( $\alpha$ -effect like)(Dikpati et al. 2004). Meridional circulation will provide a way to transport the poloidal field from the surface where it appears to the bottom of the convection zone where it is transformed into toroidal field.

---

<sup>1</sup> UMR AIM n7158, DSM/DAPNIA/SAP, CEA Saclay, 91191 Gif-Sur-Yvette Cedex

## 2 The model: equations, initial & boundary conditions & physical ingredients

To build mean field solar dynamo models, we need several ingredients such as the diffusivity profile, the expression of differential rotation and of the meridional circulation, the origin of the poloidal field source. This leads to the definition of 3 numbers  $C_\Omega = \Omega_0 R_\odot^2 / \eta_t$ ,  $C_s = s_0 R_\odot / \eta_t$  and  $R_e = v_0 R_\odot / \eta_t$  with  $\eta_t$  the turbulent diffusivity,  $\Omega_0$  the rotation rate,  $v_0$  the maximum flow speed and  $R_\odot$  the solar radius. These numbers will characterize the intensity of each effect against magnetic dissipation.

Working in spherical coordinates and under the assumption of axisymmetry, we write the total magnetic field  $\mathbf{B}$  as:

$$\mathbf{B}(r, \theta, t) = \nabla \times (A_\phi(r, \theta, t) \hat{\mathbf{e}}_\phi) + B_\phi(r, \theta, t) \hat{\mathbf{e}}_\phi, \text{ it leads to}$$

$$\frac{\partial A_\phi}{\partial t} = \eta \left( \nabla^2 - \frac{1}{\varpi^2} \right) A_\phi - \frac{\mathbf{v}_p}{\varpi} \cdot \nabla (\varpi A_\phi) + S(r, \theta, B_\phi) \quad (2.1)$$

$$\begin{aligned} \frac{\partial B_\phi}{\partial t} = & \eta \left( \nabla^2 - \frac{1}{\varpi^2} \right) B_\phi + \frac{1}{\varpi} \frac{\partial (\varpi B_\phi)}{\partial r} \frac{\partial \eta}{\partial r} - \varpi \mathbf{v}_p \cdot \nabla \left( \frac{B_\phi}{\varpi} \right) \\ & - B_\phi \nabla \cdot \mathbf{v}_p + \varpi (\nabla \times (\varpi A_\phi \hat{\mathbf{e}}_\phi)) \cdot \nabla \Omega \end{aligned} \quad (2.2)$$

where  $\varpi = r \sin \theta$ ,  $\eta$  is the magnetic diffusivity,  $\mathbf{v}_p$  the flow in the meridional plane (i.e. the meridional circulation),  $\Omega$  the differential rotation,  $S(r, \theta, B_\phi)$  the Babcock-Leighton source term for poloidal field.

Equations 2.1 and 2.2 are solved in an annular meridional cut with the colatitude  $\theta \in [0, \pi]$  and the radius  $r \in [0.6, 1] R_\odot$  i.e from slightly below the tachocline (e.g.  $r = 0.7 R_\odot$ ) up to the solar surface. At  $\theta = 0$  and  $\theta = \pi$  boundaries, both  $A_\phi$  and  $B_\phi$  are set to 0. As we assume that the radiative zone behaves as a perfect conductor, both  $A_\phi$  and  $B_\phi$  are set to 0 at  $r = 0.6 R_\odot$ . At the upper boundary,  $B_\phi = 0$  and to ensure that the radial field is not zero at the surface, we set  $\frac{\partial A_\phi}{\partial r} = 0$ . The initial conditions are the ones used in Dikpati & Charbonneau 1999, i.e the poloidal field is set to 0 whereas the toroidal field is set to  $B_0 \sin 2\theta$  above the interface and 0 below. To solve the equations, we use a code adapted by P. Charbonneau and T. Emonet in 1998 from Finite Element Analysis by D.S. Burnett. This code enables to solve a general PDE using a finite element method in space and a third order scheme in time. We adapted it to problems such as  $\alpha - \Omega$ ,  $\alpha^2 - \Omega$ , flux transport or multicellular flux transport solar dynamos.

The model "ingredients" are basically the ones used by Dikpati & Charbonneau 1999. The rotation profile is the one deduced from helioseismic inversions, assuming a solid rotation below  $0.6 R_\odot$  and a differential rotation above the interface. With this profile, the radial shear is maximal at the tachocline. In Babcock-Leighton flux transport dynamo models, the poloidal field owes its origin to the twist of the toroidal loops emerging at the solar surface. Thus, the source has to be confined in a thin layer just below the surface and as the process is fundamentally non-local, the source term depend on the variation of  $B_\phi$  at the base

of the convection zone. Moreover, a quenching term is introduced to prevent the magnetic energy from growing exponentially. We assume that the diffusivity in the envelope  $\eta_t$  is dominated by its turbulent contribution whereas in the stable zone, it is not, with  $\eta_c \ll \eta_t$ .

### 3 The results

#### 3.1 The reference unicellular model

We first consider the reference unicellular model where we assume one large single meridional cell directed poleward at the surface and we allow it to penetrate a little below the base of the convection zone. The components of the meridional flow are the ones used in Dikpati & Charbonneau 1999. With this model and parameters values of  $v_0 = 1500 \text{ cm.s}^{-1}$ ,  $s_0 = 20 \text{ cm.s}^{-1}$  and  $\eta_t = 5.10^{10} \text{ cm}^2.\text{s}^{-1}$ , we are able to reproduce several aspects of the solar cycle, especially its period of approximately 20 years here (cf. Figure 2).

#### 3.2 Introduction of a multicellular flow

To get a multicellular flow, we write the stream function  $\psi$  as a product of Chebyshev polynomials in radius and of Legendre polynomials in latitude. Through the following relations:  $\rho v_z = \frac{1}{z^2} \frac{\partial \psi}{\partial x}$  and  $\rho v_x = -\frac{1}{z\sqrt{1-x^2}} \frac{\partial \psi}{\partial z}$ , with  $z = r$ ,  $x = -\cos \theta$  and  $\rho = 1/z$ , we easily deduce the shape of the meridional flow components from the polynomial stream function. On figure 1 we plotted the 4 different stream functions.

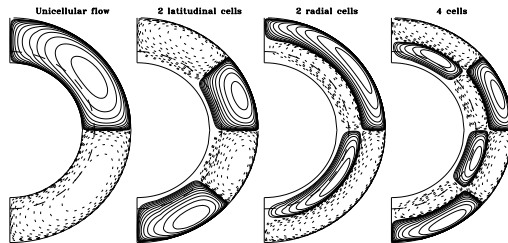


**Fig. 1.** Stream functions for the different meridional flows used in the models, solid lines representing counterclockwise circulation.

For the 4 cells model where  $\psi(x, z) = C(z - 0.6)^2(500(z - 0.8)^3 - 20(z - 0.8))(7x^5 - 10x^3 + 3x)$ , the butterfly diagram is represented on figure 2. We kept the same values of the parameters  $\eta_t$  and  $s_0$  but in order to get closer to the solar cycle period, we had to increase the maximum velocity up to  $v_0 = 3000 \text{ cm.s}^{-1}$  because this model tends to slowing down the cycle. This behavior is due to the 2 cells in radius which significantly increases the period probably because the magnetic flux is not transported from the surface to the interface as fast as it was in the unicellular model because a return flow is present at mid depth. On the

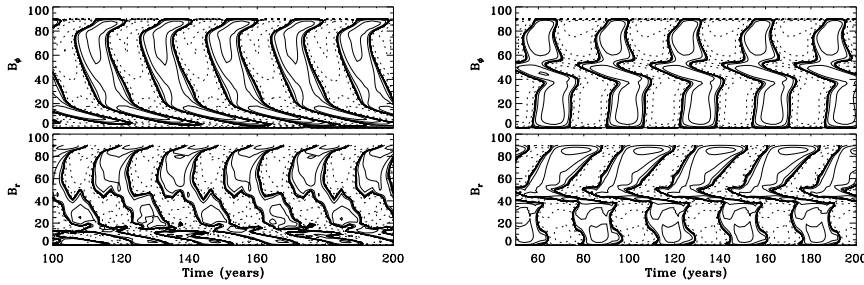


**Fig. 2.** Butterfly diagram (time-latitude cut at  $r = cst$ ) of the unicellular model (left panel) with  $v_0 = 1500 \text{ cm.s}^{-1}$  and of the 4 cells BL flux transport dynamo model (right panel) with  $v_0 = 3000 \text{ cm.s}^{-1}$ . The contours of  $B_\phi$  are plotted at the base of the convection zone and  $B_r$  is taken at the surface. Contours are logarithmically spaced with 2 contours covering a decade in field strength and solid lines represent positive values of the field.

contrary, adding cells in latitude decreases the time for the fluid to travel along the conveyor belt, hence the flux is transported faster from the surface to the base of the convection zone and thus the regeneration of each component of the magnetic field is faster, as shown by Dikpati et al. 2004 and Bonanno et al. 2005.

### 3.3 Perspectives and future improvements

As we said before, one of the major improvements in these models would be to modify the boundary conditions so  $A_\phi$  could be smoothly matched with an exterior potential field (Dikpati & Choudhuri 1995). Moreover, models with only a surface term fail to reproduce the dipolar symmetry of the toroidal field in the long term but the lack of such a bottom  $\alpha$  effect does not seem to change our conclusion on the impact of multicellular meridional circulation flow on setting the cycle period and slowing down with multi cells in radius.

## References

- Bonanno et al., 2005, *Astronomische Nachrichten*, 326, 170
- Brun, A.S, Miesch, M.S. & Toomre J. 2004, *ApJ*, 614, 1073
- Burnett, D.S., 1987, *Finite Element Analysis*, Addison-Wesley
- Charbonneau, P., 2005, *Living Rev. Solar Phys.*, 2
- Dikpati et al., 2004, *ApJ*, 601, 1136-1151
- Dikpati, M. & Charbonneau, P., 1999, *ApJ*, 518, 508
- Dikpati, M. & Choudhuri, A.R., 1994, *Astron. Astrophys.*, 291, 975-989
- Thompson et al., 2003, *ARA&A*, 41, 599